

Ferromagnetism in pure wurtzite zinc oxide

Xu Zuo,^{1,a)} Soack-Dae Yoon,² Aria Yang,² Wen-Hui Duan,³ Carmine Vittoria,² and Vincent G. Harris²

¹College of Information Technical Science, Nankai University, Tianjin 300071, People's Republic of China

²Department of Electrical and Computer Engineering, Northeastern University, Boston, Massachusetts 02115, USA

³Department of Physics, Tsinghua University, Beijing, 100084, People's Republic of China

(Presented 13 November 2008; received 6 September 2008; accepted 25 October 2008; published online 5 February 2009)

The ferromagnetism induced by the intrinsic point defects in wurtzite zinc oxide is studied by using *ab initio* calculation based on density functional theory. The calculations show that both oxygen interstitial and zinc vacancy may induce ferromagnetism into this material. The calculations also show that zinc oxide with oxygen interstitial may be a ferromagnetic semiconductor. Based on the simplified electronic configuration of the defect molecules, we explain the total magnetic moment, electronic structure, and ferromagnetism. © 2009 American Institute of Physics.

[DOI: 10.1063/1.3062822]

The discovery of unexpected magnetism in HfO₂ thin film¹ has triggered a debate on the origins of the ferromagnetism in the undoped diamagnetic oxide. Experiments have shown that ferromagnetism may be universal in the nanoparticles² or films^{3,4} of diamagnetic oxides. Moreover, *ab initio* calculations have predicted that ferromagnetism may be induced by Hf vacancy in HfO₂,⁵ or by O vacancy in TiO₂.⁶ In the diamagnetic oxides showing *d*⁰-magnetism, zinc oxide (ZnO) has drawn great interest. Experiments have discovered room-temperature ferromagnetism in undoped ZnO nanoparticles⁷ and films,⁸ and in carbon-doped ZnO films.⁹ Moreover, *ab initio* calculations have shown that magnetism may be induced by C substitution in ZnO,⁹ or by Zn vacancy in zinc chalcogenides with zinc blende structure.¹⁰ In this paper, we study the ferromagnetism induced by the intrinsic point defects in wurtzite ZnO (*w*-ZnO) using *ab initio* calculation based on density functional theory. We choose wurtzite structure because most films and nanoparticles of ZnO prepared in the experiments are in this structure.

The *ab initio* calculations are performed on the defect supercells, which are derived from the prototypical supercell by removing (or adding) a Zn (or O) atom. The prototypical supercell is a 2 × 2 × 2 supercell consisting of 16 chemical formulas (Zn₁₆O₁₆). The calculation is performed in two steps: the structural relaxation is followed by the calculation of properties. In the first step, both lattice parameters and atomic positions are relaxed by using Perdew-Wang 91 (PW91) generalized gradient approximation (GGA) exchange correlation and ultrasoft pseudopotential. This step is numerically accomplished by the VASP code with a 4 × 4 × 3 *k*-mesh and the accuracy up to 10⁻³ and 10⁻⁴ eV for the ionic and electronic loops, respectively. In the second step, electronic structure and magnetic properties are calculated by using Perdew-Burke-Ernzerhof (PBE) GGA exchange-correlation and full-potential linear augmented plane wave

method. This step is numerically accomplished by the WIEN2K code with a 5 × 5 × 3 *k*-mesh and the accuracy up to 10⁻⁶ Ry. In both steps, the spin polarization options are enabled.

We investigate oxygen vacancy (*V*_O), oxygen interstitial (*I*_O), zinc vacancy (*V*_{Zn}), and zinc interstitial (*I*_{Zn}) as the possible sources of the magnetic moment.¹¹ We depict the relaxed local structures in Fig. 1, where the *I*_O is located inside a cage-shaped Zn₆O₆ molecule and the *V*_{Zn} is located inside a tetrahedral O₄ molecule. For the convenience of further discussion, we define the defect molecule consisting of the defect and the first-shell O ions. The defect molecule is an octahedral O₇ molecule for *I*_O or a tetrahedral O₄ molecule for *V*_{Zn}.

The total and site-projected magnetic moments are estimated from the spin populations. The total magnetic moments of *I*_{Zn} and *V*_O vanish, but those of *I*_O and *V*_{Zn} are 2.00 and 1.77 μ_B, respectively (Table I). In both cases of *I*_O and *V*_{Zn}, there is little magnetic moment in the interstitial region or on the Zn ions, and most of the magnetic moment is

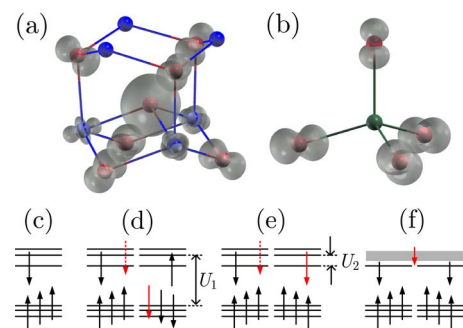


FIG. 1. (Color online) (a) and (b) show the relaxed local structures and spin isosurfaces of *I*_O and *V*_{Zn}, respectively. The O, Zn, and *V*_{Zn} are colored red, blue, and green, respectively. (c) shows the simplified electronic configuration for the defect molecules. (d)–(f) show the antiferromagnetic and ferromagnetic superexchanges, and double exchange, respectively. The impurity band corresponding to the minority LUMO of the defect molecule is colored gray in (f).

^{a)}Electronic mail: xzuonku@gmail.com.

TABLE I. Summary of the calculated results. m is the total magnetic moment per supercell. $\Delta E_1 = E_{DM} - E_{FM}$ is the energy difference between the diamagnetic and ferromagnetic states. $\Delta E_2 = E_{AFM} - E_{FM}$ is the energy difference between the antiferromagnetic and ferromagnetic states.

	m (μ_B)	ΔE_1 (meV)	ΔE_2 (meV)
I_O	2.00	18.83	1.21
V_{Zn}	1.77	7.67	4.77

localized on the defect molecule. To visualize the detailed distribution of magnetic moments, we plot the calculated spin isosurfaces in Fig. 1. The distributions of magnetic moment strongly suggest that the magnetic moment is originated from the O- p orbitals of the defect molecules.

To examine the stability of the local magnetic state, we calculate the energy difference between the diamagnetic and ferromagnetic states. The energy differences show that in both cases of I_O and V_{Zn} the ferromagnetic state is more stable than the diamagnetic state (Table I). To examine the exchange coupling between the defect molecules, we calculate the energy difference between the antiferromagnetic and ferromagnetic states (Table I). To do the calculation, we induce two I_O (or V_{Zn}) in the prototypical supercell. We first relax the structure, and then calculate the total energies of the ferromagnetic and antiferromagnetic states, respectively. In both cases of I_O and V_{Zn} , the ferromagnetic state is lower in energy than the antiferromagnetic state, which suggests that exchange coupling between the defect molecules is ferromagnetic.

We calculate the density of states (DOS) of w -ZnO with I_O and V_{Zn} , respectively, and plot them in Fig. 2. We also calculate the DOS for perfect w -ZnO as the reference. In both cases, the defect induces the impurity bands around the Fermi level. The projected DOS shows that the impurity bands are mainly formed by the O- p orbitals of the defect molecule. In the case of V_{Zn} , the DOS is a ferromagnetic metal, where both majority and minority DOS at the Fermi level are nonzero but not equal to each other. In the case of I_O , the DOS is a ferromagnetic semiconductor, where the minority band gap is much narrower than the majority one.

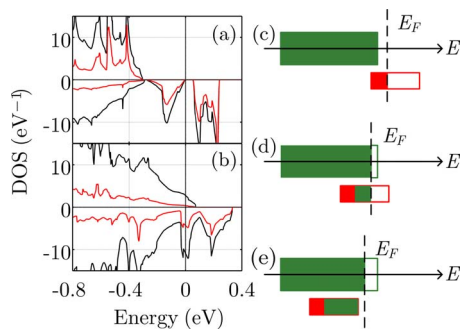


FIG. 2. (Color online) (a) and (b) show the DOS of w -ZnO with I_O and V_{Zn} , respectively. The black and red lines are the total DOS and the DOS projected to the O- p orbitals of the defect molecule, respectively. The Fermi level is aligned to 0 eV. (c)–(e) show three cases depending on the position of the impurity band corresponding to the minority HOMO relative to the host VBM. The host valence band and the impurity bands induced by the defect molecule are colored green and red, respectively.

As the defect molecules may play the key role in the d^0 -magnetism of w -ZnO, we perform *ab initio* calculations to study the electronic configurations of the defect molecules. The calculations are performed on the defect molecules, O_7 molecule in the case of I_O and O_4 molecule in the case of V_{Zn} . To simulate the charge-compensating effect in the solid, the O_7 molecule is charged as O_7^{-12} and the O_4 molecule as O_4^{-6} . The calculations are performed by using Becke-Lee-Yang-Parr (BLYP) GGA exchange-correlation and double numerical plus d -functions basis set, and numerically accomplished by the DMOL3 code with the accuracy up to 10^{-6} Hartree.

In the calculation, we first ignore the structural relaxation temporarily. Thus, the defect molecule is in high symmetry O_h for I_O (or T_d for V_{Zn}). The spin-restricted calculation shows that the highest occupied molecular orbital (HOMO) is triply degenerated T_{1u} for I_O (or T_2 for V_{Zn}). Since two electrons are removed from the defect molecule due to the charge-compensating effect, the HOMO is partially occupied by four electrons. The spin-unrestricted calculation shows that the majority and minority levels will split. The majority levels will be fully occupied by three electrons and the minority levels will be partially occupied by one electron. Thus, the defect molecule exhibits a magnetic moment of $2\mu_B$. When the relaxed structure given by the supercell approach is used in the calculation, the degeneration of the majority (or minority) levels will be lifted. The simplified electronic configuration is depicted in Fig. 1(c). For the convenience of further discussion, we denote the energy difference between the majority HOMO and the minority lowest unoccupied molecular orbital (LUMO) as U_1 and that between the minority HOMO and LUMO as U_2 .

By comparing the simplified electronic configuration [Fig. 1(c)] to the DOS [Figs. 2(a) and 2(b)], it is obvious that the three minority levels in the simplified electronic configuration are corresponding to the minority impurity bands around the Fermi level. Thus, we may explain the total magnetic moment, electronic structure, and ferromagnetism based on the simplified electronic configuration.

In the case of I_O , the impurity band corresponding to the minority HOMO is higher than the valence band maximum (VBM) [Fig. 2(c)]. The electron occupation of the defect molecule will hold true. Thus, the total magnetic moment is $2\mu_B$. The spin-unrestricted calculation using the relaxed structure given by the supercell approach shows that $U_2 \sim 0.5$ eV for the O_7 molecule. The large U_2 of the O_7 molecule results in the minority band gap in the DOS [Fig. 2(a)]. Thus, w -ZnO with I_O is a ferromagnetic semiconductor.

The ferromagnetism of w -ZnO with I_O may be attributed to the superexchange interactions between the defect molecules. The simplified electronic configuration implies both ferromagnetic and antiferromagnetic superexchanges between the defect molecules.¹² The virtual transfer between the occupied majority (or minority) levels of a defect molecule and the unoccupied minority levels of another defect molecule will result in antiferromagnetic (or ferromagnetic) superexchange [Figs. 1(d) and 1(e)]. The dominant contribution to the antiferromagnetic (or ferromagnetic) superexchange is due to the virtual transfer between the majority (or

minority) HOMO and the minority LUMO. The spin-unrestricted calculation using the relaxed structure given by the supercell approach shows that the spatial distributions of the minority and majority HOMOs are almost identical, which implies that the transfer integrals corresponding to the dominant ferromagnetic and antiferromagnetic superexchanges are approximately equal. Thus, the relative strength of the dominant superexchange interactions will be determined by the effective on-site Coulomb repulsion energies, which are U_1 and U_2 for the antiferromagnetic and ferromagnetic superexchanges, respectively.¹³ We estimate $U_1 \sim 0.5$ eV and $U_2 \sim 0.25$ eV from the DOS [Fig. 2(a)]. Thus, the dominant ferromagnetic superexchange is about two times stronger than the dominant antiferromagnetic superexchange. As a result, the total superexchange interaction between the defect molecules is ferromagnetic in w -ZnO with I_O .

In the case of V_{Zn} , the impurity band corresponding to the minority HOMO is lower than the VBM (but not too much) [Fig. 2(d)]. The electrons will relocate from the host valence band (both majority and minority) to the minority impurity band corresponding to the minority LUMO of the defect molecule. Thus, the total magnetic moment is less than $2\mu_B$. If the impurity bands are much lower than the VBM, the total magnetic moment will vanish due to the relocation of electrons [Fig. 2(e)]. The relocation results in the finite spin densities in both majority and minority directions at the Fermi level in the DOS [Fig. 2(b)]. Thus, w -ZnO with V_{Zn} is a ferromagnetic metal.

The ferromagnetism of w -ZnO with V_{Zn} may be attributed to the double exchange interaction between the defect molecules. In fact, the impurity band corresponding to the minority LUMO in the DOS [Fig. 2(b)] is partially filled due to the relocation. In another picture, the minority spins itinerate between the LUMOs of the defect molecules and interact with the local spins via the on-site exchange interaction [Fig. 1(f)]. As a result, the local magnetic moments of the defect molecules are aligned up by the itineration. We may also understand the ferromagnetism of w -ZnO with V_{Zn} following the idea of charge-transfer ferromagnetism.¹⁴ The charge reservoir in our case is the host instead of the doped

ocations. The relocation (or transfer) of electrons from the host valence band to the impurity bands raises the Fermi level to the peak of DOS corresponding to the LUMO, which results in Stoner split of the impurity bands and, consequently, the spontaneous Stoner ferromagnetism.

In conclusion, we have shown by *ab initio* calculation that both I_O and V_{Zn} may induce ferromagnetism in w -ZnO. However, w -ZnO with V_{Zn} is a ferromagnetic metal and w -ZnO with I_O is a ferromagnetic semiconductor. We have proposed the simplified electronic configuration for the defect molecules, based on which we have explained the calculated results including the total magnetic moment, electronic structure, and ferromagnetism.

This research was sponsored by the China National Science Foundation (Grant No. 60601001), the Ministry of Education (Grant No. NCET-06-0219), the Ministry of Science and Technology (Grant No. 2006CB605105), and the NKStar HPC program.

- ¹M. Venkatesan, C. Fitzgerald, and J. Coey, *Nature (London)* **430**, 630 (2004).
- ²A. Sundaresan, R. Bhargavi, N. Rangarajan, U. Siddesh, and C. N. R. Rao, *Phys. Rev. B* **74**, 161306 (2006).
- ³S. Yoon, Y. Chen, A. Yang, T. Goodrich, X. Zuo, D. Arena, K. Ziemer, C. Vittoria, and V. Harris, *J. Phys.: Condens. Matter* **18**, L355 (2006).
- ⁴N. Hong, J. Sakai, N. Poirot, and V. Brize, *Phys. Rev. B* **73**, 132404 (2006).
- ⁵C. Das Pemmaraju and S. Sanvito, *Phys. Rev. Lett.* **94**, 217205 (2005).
- ⁶X. Zuo, S.-D. Yoon, A. Yang, C. Vittoria, and V. G. Harris, *J. Appl. Phys.* **103**, 07B911 (2008).
- ⁷S. Banerjee, M. Mandal, N. Gayathri, and M. Sardar, *Appl. Phys. Lett.* **91**, 182501 (2007).
- ⁸Q. Xu, H. Schmidt, S. Zhou, K. Potzger, M. Helm, H. Hochmuth, M. Lorenz, A. Setzer, P. Esquinazi, Ch. Meinecke, and M. Grandmann, *Appl. Phys. Lett.* **92**, 082508 (2008).
- ⁹H. Pan, J. B. Yi, L. Shen, R. Q. Wu, J. H. Yang, J. Y. Lin, Y. P. Feng, J. Ding, L. H. Van, and J. H. Yin, *Phys. Rev. Lett.* **99**, 127201 (2007).
- ¹⁰T. Chanier, I. Opahle, M. Sargolzaei, R. Hayn, and M. Lannoo, *Phys. Rev. Lett.* **100**, 026405 (2008).
- ¹¹S. Lany and A. Zunger, *Phys. Rev. Lett.* **98**, 045501 (2007).
- ¹²W. Anderson, *Phys. Rev.* **115**, 2 (1959).
- ¹³B. Belhadji, L. Bergqvist, R. Zeller, P. H. Dederichs, K. Sato, and H. Katayama-Yoshida, *J. Phys.: Condens. Matter* **19**, 436227 (2007).
- ¹⁴J. M. D. Coey, K. Wongsaprom, J. Alaria, and M. Venkatesan, *J. Phys. D: Appl. Phys.* **41**, 134012 (2008).